

ATOMIC ABSORPTION PROFILES ASSOCIATED WITH PULSED EXCITATION

N.V. VITANOV^{1,2}, B.W. SHORE³, L.P. YATSENKO⁴

UDC 535.342

© 2009

¹Department of Physics, Sofia University
(James Boucher 5 blud., 1164 Sofia, Bulgaria),

²Institute of Solid State Physics, Bulgarian Academy of Sciences
(Tsarigradsko chaussée 72, Sofia 1784, Bulgaria),

³Fachbereich Phys. Techn. Universität
(Kaiserslautern D-67663, Germany),

⁴Institute of Physics, Nat. Acad. of Sci. of Ukraine
(46, Nauki Prosp., Kiev-39, 03650, Ukraine)

The spectral width of an atomic absorption line, observed with a steady (cw) coherent light source, typically increases in proportion to the square root of the light intensity, an effect known as the power broadening. We show that such an excitation, as monitored by the fluorescence signal, differs qualitatively when the excitation is pulsed. We consider the variation of the fluorescence (summed over all frequencies) with the frequency of an excitation-producing laser and show that the associated excitation profile contains two components: a power-broadened one and a narrow line, whose width depends mainly on the natural width and only very weakly on the laser intensity. Unlike the signal produced with photoionization with a continuous ionization field [Halfmann *et al.*, Opt. Commun. **220**, 353 (2003)], the width of the narrow line does not depend on the pulse duration.

how the photoionization measurement is made: the measurements performed *during* the excitation exhibit the power broadening (a width proportional to the Rabi frequency of the excitation step), whereas the measurements performed *after* the excitation do not [5, 6].

The present paper presents another important type of the frequency-dependent excitation feature (an *excitation profile*), one that appears in measurements of the fluorescence (spontaneous emission) from an excited state to the ground state. Specifically, we consider the *total fluorescence* signal collected during a pulsed excitation – the integral over all frequencies present in the fluorescence.

Similar to the earlier description of the photoionization associated with a pulsed excitation, we identify two components in the profile: one is power-broadened (a width proportional to the Rabi frequency), while the other has a width that depends mainly on the natural width and only weakly on the Rabi frequency. However, unlike a similar structure observed with photoionization, the width of the narrow feature observed in fluorescence does not depend on the pulse duration.

This paper is organized as follows. In Section 2, we define a function, the *excitation profile* $\mathcal{S}(\Delta)$ that presents the expected distribution of a fluorescence signal as a function of Δ , the frequency separation of the excitation field from the resonance. We consider three scenarios for the excitation and the measurement, each capable of producing an excitation profile.

In Section 3, we use the Bloch equations to model elements of the density matrix needed to evaluate the fluorescence. We relate the relevant excitation profile function to elements of the density matrix. To assist

1. Introduction

Observations of radiation attenuation by vapor display a well-known absorption profile of transmitted intensity varying with the incident radiation frequency – a spectral line. The width of such a spectral line is affected by several factors, e.g. spontaneous emission (*natural broadening*), atomic motion (*Doppler broadening*), and vapor density (*pressure broadening* induced by collisions) [1, 2]. The details of the frequency variation – the line profile – are also affected by the radiation intensity (*power broadening*) [3, 4]. However, the power broadening does not always occur: as we shall illustrate, its extent depends critically upon the nature of the excitation step and the type of measurement.

An earlier paper demonstrated this sensitivity theoretically and experimentally, by considering the photoionization signal produced from the excited state as a function of the frequency of the excitation-producing field. The variation of this signal with frequency, regarded as a spectral line, depends on

in the analysis of power-broadening effects, we define a frequency-dependent effective line width $\mathcal{D}(\Delta)$.

Section 4 presents analytic expressions for the excitation profile and the derived effective linewidth for several simple models of temporal pulse envelopes. We comment on these results in Section 5.

2. Examples of Excitation Profiles

2.1. Steady-state excitation by a cw laser

Before treating the pulsed excitation, it is helpful to review the origin of power broadening as produced by the cw excitation of a fluorescing atom. As a model of the emission line, we consider the total steady fluorescence (i.e. the integral over emitted frequencies) from an ensemble of identical two-state atoms irradiated by a cw laser, whose frequency ω is varied around the atomic Bohr frequency ω_0 , as measured by the detuning $\Delta \equiv \omega_0 - \omega$. The spontaneous emission rate from the excited state is taken to be Γ , and the laser-atom interaction is quantified by the Rabi frequency [7] $\Omega = -\mathbf{d} \cdot \mathbf{E}/\hbar$ which is proportional to the projection of the transition dipole moment \mathbf{d} on the laser electric field \mathbf{E} . The dependence of the fluorescence signal on Δ defines, apart from normalization, the *excitation profile*, $\mathcal{S}(\Delta)$.

Because the fluorescence appears from the spontaneous emission from excited atoms, the fluorescence signal is proportional to the time-averaged excited-state population. We use the density matrix $\rho(t)$ to define the excitation profile as [5, 6]

$$\mathcal{S}_{\text{cw}}(\Delta) = \langle \rho_{22}(t) \rangle \equiv \lim_{T \gg \Gamma^{-1}} \frac{1}{T} \int_0^T \rho_{22}(t) dt. \quad (1)$$

From the well-known solutions to the Bloch equations [3], it follows that [3]

$$\mathcal{S}_{\text{cw}}(\Delta) = \frac{\Omega^2/4}{\Delta^2 + \Gamma^2/4 + \Omega^2/2}. \quad (2)$$

Thus, the excitation profile defined in this way is a Lorentzian function of Δ , with a half-width at the half-maximum (HWHM) given by

$$\Delta_{1/2} = \frac{1}{2} \sqrt{\Gamma^2 + 2\Omega^2}. \quad (3)$$

When the Rabi frequency is much larger than the natural line width ($\Omega \gg \Gamma$), the line width grows linearly with the Rabi frequency, $\Delta_{1/2} \approx \Omega/\sqrt{2}$; hence, such spectra exhibit the typical power broadening.

2.2. Pulsed excitation and delayed pulsed measurement

A different type of the profile is observed for the pulsed excitation when the signal (photoionization or fluorescence) is observed *after* the excitation. Let the signal be observed at time t_f , after the pulse but before the excited state can decay radiatively, $\Gamma t_f \ll 1$. This signal originates in the excited state population, as it exists at the end of the pulse,

$$\mathcal{S}_{\text{pulsed}}(\Delta) = \rho_{22}(t_f). \quad (4)$$

Such situations take place, for example, when the excitation occurs as an atom moves across a stationary laser beam; the characteristic pulse duration is the beam waist divided by the atom velocity.

The pulse-produced excitation $\rho_{22}(t_f)$ depends very significantly upon the properties of the pulse. Unless the carrier frequency ω is very close to the resonance with the Bohr frequency ω_0 , then a sufficiently smooth pulse (e.g., an atom moving sufficiently slowly through the laser beam) will produce the complete *coherent population return* (CPR): after a transient excursion to the excited state, all population will return to the ground state, from which no signal occurs. Under these conditions, CPR, fluorescence will only occur for small detunings, i.e. at the center of the spectral line. A typical measure of “small” in this context is the inverse of the Fourier bandwidth of the pulse, typically $\Delta_0 = C/T$, where T is the pulse duration and C is a parameter of order of unity that depends on the temporal shape of the pulse. (Some intensity-dependent correction to this simple estimate is needed [5,6].) Thus, the measurements performed *after* a pulsed excitation will exhibit almost no power broadening [5, 6]. For example, a hyperbolic-secant pulse produces CPR for $\Delta T > 1$, and there is no power broadening at all for such pulses [5, 6, 9]. For a Gaussian pulse, there is a weak logarithmic dependence of the spectral width on the Rabi frequency [10].

Although the signals produced after a pulsed excitation can exhibit a little power broadening, the duration of the pulse can have a significant effect. Because the bounding detuning for CPR is Δ_0 , the excitation profile width is proportional to $1/T$. Therefore, the spectral width increases with decrease in the pulse duration, which is an example of the *transit time* broadening. The following section presents some examples, in which such a broadening appears.

2.3. Pulsed excitation and steady measurement

As discussed in the earlier paper [5], a photoionization signal may be produced by a pulsed pump field and a steady probe field. Similarly, the fluorescence occurs during the pulsed excitation and afterwards. The signal collected *during* the action of a pump pulse samples the average excitation $\langle \rho_{22}(t) \rangle$. When the pulse is present, the width of the excitation profile increases with the Rabi frequency; hence, such a signal will exhibit the power broadening. However, the signal collected *after* is affected by the CPR discussed in Section 2, and so it will exhibit a little power broadening. Thus, one will observe a combination of the narrow feature with a width proportional to $1/T$ and the power-broadened feature with a width determined by the pump Rabi frequency [5, 6]. The present paper deals with conditions such that all the fluorescence occurs only during a pulse. The decay is sufficiently rapid, so that the excitation ceases once the pulse terminates.

2.4. Comments

In the present paper, we are concerned with the absorption of radiation, as signalled by excitation, not with the distribution of frequencies that occur in the fluorescence. Therefore, we employ a simple two-state model of the atom expressed by the Bloch equations that include the spontaneous emission and consider steady-state solutions.

This steady-state model provides a description of the atomic dynamics that is useful for understanding the excitation step, and its dependence on the carrier frequency of a laser producing the excitation, as monitored by the photoionization or fluorescence. The fluorescence radiation has its own distribution of frequencies. A spectroscopist collecting the fluorescence passes this radiation through a spectrometer to determine the traditional *emission spectrum*. The totality of this fluorescence radiation, into all solid angles and integrated over all frequencies, is proportional to the product of the emission rate A and the excited state population. The simple Bloch-vector model presented here does not give a description of the fluorescence spectrum. When the laser field becomes sufficiently strong, so that Rabi oscillations dominate the atom dynamics – coherent excitation – the periodic variation of the dipole moment creates sidebands to the fluorescent signal. These are offset from the carrier frequency and are separated by the Rabi frequency. The spectrum appears as a *Mollow triplet* [11].

The treatment of such observations requires a more elaborate treatment than the simple average excitation probability used here.

3. Excitation Profiles for Pulsed Excitation

The excitation profiles for the pulsed excitation discussed above do not involve the spontaneous emission from an excited state to the ground state during the action of a pulse. The spontaneous emission has only been included for the cw excitation in the steady-state regime, Section 2.. It is therefore of interest to consider the important case where the signal is collected during the pulsed excitation. This problem is our main interest in the present work. Specifically, we consider pulse durations T much longer than the spontaneous-emission lifetime of the excited state, $1/\Gamma$, so that many optical pumping cycles occur.

3.1. Excitation profile in the steady-state regime

When one measures the total laser-induced fluorescence during the excitation, the signal (essentially the number of emitted photons) is proportional to the time-integrated excited state population. Omitting any consideration of the detection efficiency, we define the excitation profile to be

$$S(\Delta) = \int_{-\infty}^{+\infty} \rho_{22}(t) dt. \quad (5)$$

The excited-state population $\rho_{22}(t)$ can be derived from the optical Bloch equations for a closed two-state system [7],

$$\dot{u} = -\frac{\Gamma}{2}u - \Delta v, \quad (6a)$$

$$\dot{v} = \Delta u - \frac{\Gamma}{2}v - \Omega w, \quad (6b)$$

$$\dot{w} = \Omega v - \Gamma(w + 1), \quad (6c)$$

where $u \equiv 2\text{Re}\rho_{12}$, $v \equiv 2\text{Im}\rho_{12}$ and $w \equiv \rho_{22} - \rho_{11}$ are the components of the Bloch vector. For a sufficiently long pulse duration T such that many excitation-emission cycles take place,

$$\Gamma T \gg 1, \quad (7)$$

the Bloch vector reaches an equilibrium such that its components steadily follow the conditions set by the

Rabi frequency. We assume this scenario expressed by the conditions $\dot{u}, \dot{v}, \dot{w} \approx 0$. The solutions then read

$$w = -\frac{\Delta^2 + (\Gamma/2)^2}{\Delta^2 + (\Gamma/2)^2 + \Omega^2/2}, \quad (8a)$$

$$u = -\frac{\Delta}{\Gamma/2}v, \quad (8b)$$

$$v = -\frac{\Omega(\Gamma/2)}{\Delta^2 + (\Gamma/2)^2}w. \quad (8c)$$

It follows from these formulas that the steady-state population of the excited state is

$$\rho_{22}(t) = \frac{w(t) + 1}{2} = \frac{\Omega^2(t)/4}{\Delta^2 + (\Gamma/2)^2 + \Omega^2(t)/2}, \quad (9)$$

and that the excitation profile is

$$S(\Delta) = \frac{\Gamma}{2} \int_{-\infty}^{+\infty} \frac{\Omega^2(t)/2}{\Delta^2 + (\Gamma/2)^2 + \Omega^2(t)/2} dt. \quad (10)$$

This function provides different excitation profiles for different pulse shapes $\Omega(t)$. The following section provides several examples. In what follows, we consider the saturation regime, in which the coherent interaction dominates the incoherent spontaneous emission in the excitation, $\Omega_0 \gg \Gamma$.

3.2. Effective line width

For the pulsed excitation, the excitation profile given by Eq. (10) is not Lorentzian and can have a rather complicated shape. In order to characterize the spectrum in a most simple way, it is convenient to define an effective frequency-dependent width (HWHM) $\mathcal{D}(\Delta)$ by writing the excitation profile as

$$S(\Delta) = \frac{S(0)}{1 + \left[\frac{\Delta}{\mathcal{D}(\Delta)} \right]^2}. \quad (11)$$

The effective width so defined is obtained from the formula

$$\mathcal{D}(\Delta) = |\Delta| \left(\frac{S(0)}{S} - 1 \right)^{-1/2}. \quad (12)$$

The following section presents examples of the effective width $\mathcal{D}(\Delta)$ deduced for several pulse shapes. We comment there on the behavior of this function for small Δ (near the line center) and for large Δ (the wings of the line).

4. Examples of Temporal Pulses

This section presents several examples of pulses, for which analytic expressions can be obtained for the excitation profile and the associated effective line width. From these examples, we draw some general conclusions.

4.1. Rectangular pulse

The simplest manifestation of the power broadening is evident from a rectangular pulse of duration T ,

$$\Omega(t) = \begin{cases} \Omega_0, & 0 \leq t \leq T, \\ 0, & \text{elsewhere.} \end{cases} \quad (13)$$

The excitation profile predicted for this pulse is

$$S(\Delta) = \frac{\Omega_0^2 T/4}{\Delta^2 + \Gamma^2/4 + \Omega_0^2/2}. \quad (14)$$

This is a Lorentzian profile, and so the effective width is independent of Δ ; it is

$$\mathcal{D}(\Delta) = \frac{1}{2} \sqrt{\Gamma^2 + 2\Omega_0^2} \approx \begin{cases} \Omega_0/\sqrt{2}, & (\Omega_0 \gg \Gamma), \\ \Gamma/2, & (\Omega_0 \ll \Gamma). \end{cases} \quad (15)$$

Once the Rabi frequency exceeds the natural linewidth Γ , this expression exhibits a nearly linear dependence on the Rabi frequency, i.e. the excitation profile exhibits the conventional power broadening in the wings.

4.2. Gaussian pulse

Typically, atoms moving transversely across laser beams encounter a Gaussian spatial variation of the laser intensity and hence experience a Gaussian pulse. Thus, it is important to consider how observations of the fluorescence from such pulses would alter the excitation profile, as defined here. For the pulse

$$\Omega(t) = \Omega_0 \exp(-t^2/T^2), \quad (16)$$

the excitation profile is expressible as

$$S(\Delta) = \frac{1}{2} \int_{-\infty}^{+\infty} \frac{1}{1 + \alpha^2 \exp(2t^2/T^2)} dt = \frac{T}{\sqrt{2}} I(\alpha), \quad (17)$$

where

$$\alpha^2 \equiv \frac{\Delta^2 + \Gamma^2/4}{\Omega_0^2/2}, \quad (18)$$

and $I(\alpha)$ is the integral

$$I(\alpha) = \int_0^{+\infty} \frac{dx}{\alpha^2 \exp(x^2) + 1}. \quad (19)$$

The integral $I(\alpha)$ cannot be calculated exactly, but we can approximate it using the following observations.

The integrand $f(x) = 1/(\alpha^2 e^{x^2} + 1)$ is a monotonically decreasing function of x which has its maximum $f_{\max} = f(0) = 1/(\alpha^2 + 1)$ at $x = 0$. We approximate the integral by replacing the integrand $f(x)$ by its maximum value f_{\max} while shrinking the integration interval from $[0, \infty)$ to $[0, x_0]$, where x_0 is, for the moment, a free parameter. To justify this simplification, we argue that the error from the neglected contribution from the interval $[x_0, \infty)$ can be compensated by the error from the overestimation of the function $f(x)$ by its maximum $f_{\max} = 1/(\alpha^2 + 1)$ in the interval $[0, x_0]$.

We choose x_0 to be the point, at which $f(x)$ decreases to f_{\max}/n , where n is still to be fixed. Then integral (19) is approximated as

$$I(\alpha) \approx \frac{x_0}{1 + \alpha^2} = \frac{1}{1 + \alpha^2} \sqrt{\ln \left(n + \frac{n-1}{\alpha^2} \right)}. \quad (20)$$

Obviously, for each α , the parameter x_0 or n can be chosen in such a way that Eq. (20) provides the exact result. Then, however, x_0 and n will be functions of α , and this determination is equivalent to the calculation of the integral $I(\alpha)$. We can fix the value of n by requiring that approximation (20) provide the exact result for $\alpha = 1$. This occurs for the value

$$n = 2.07833\dots \quad (21)$$

The excitation profile defined by Eq. (17) is

$$\mathcal{S}(\Delta) = \frac{\sqrt{2}\Omega_0^2 T/8}{\Delta^2 + \Gamma^2/4 + \Omega_0^2/2} \sqrt{\ln [n + (n-1)\beta^2]}, \quad (22)$$

where

$$\beta^2 \equiv \frac{(n-1)\Omega_0^2/2}{\Delta^2 + \Gamma^2/4}. \quad (23)$$

The effective line width is, with $\beta_0 \equiv \Omega_0\sqrt{2}/\Gamma$,

$$\mathcal{D}(\Delta) = \Delta \left[586 \left(1 + \frac{\Delta^2}{\Gamma^2/4 + \Omega_0^2/2} \right) \times \right.$$

$$\left. \times \sqrt{\frac{\ln [n + (n-1)\beta_0^2]}{\ln [n + (n-1)\beta^2]} - 1} \right]^{-1/2}. \quad (24)$$

For small detunings, the line width is primarily determined by the natural width Γ ,

$$\mathcal{D}(\Delta) \approx \Gamma \sqrt{\ln \left(\sqrt{2(n-1)}\Omega_0/\Gamma \right)}, \quad (|\Delta| \ll \Gamma \ll \Omega_0). \quad (25a)$$

For intermediate detunings, the expression becomes

$$\mathcal{D}(\Delta) \approx |\Delta| \sqrt{\frac{\ln(\Omega_0/\sqrt{2})}{\ln(2|\Delta|/\Gamma)}}, \quad (\Gamma \ll |\Delta| \ll \Omega_0). \quad (25b)$$

For large Δ , the width is determined by the peak Rabi frequency Ω_0 ,

$$\mathcal{D}(\Delta) \approx \Omega_0 \sqrt[4]{\frac{\ln n}{8 \ln \left[\sqrt{2(n-1)}\Omega_0/\Gamma \right]}}, \quad (\Gamma \ll \Omega_0 \ll |\Delta|). \quad (25c)$$

Figure 1 presents a comparison of the excitation profiles of Gaussian and square pulses for three values of the peak Rabi frequency. In the first of these (top frame), the peak Rabi frequency is equal to Γ . We would not expect to see the power broadening, and, indeed, the expectation is confirmed by the profile. In the middle frame, the peak Rabi frequency is larger. Here, we see that the square pulse (R) has noticeably broadened the central portion of the profile, whereas the Gaussian pulse (G) has primarily produced broader profile wings. In the bottom frame, the peak Rabi frequency is larger still, and the difference between the two profiles is even more noticeable: the central portion of the excitation profile produced by a Gaussian pulse has broadened much less than the profile related to a rectangular pulse, which grows in width proportionally to the square root of the peak Rabi frequency.

4.3. Hyperbolic secant pulse

The comparisons shown in Fig. 1 show that different temporal pulse shapes can produce very different excitation profiles. The hyperbolic secant pulse,

$$\Omega(t) = \Omega_0 \operatorname{sech}(t/T), \quad (26)$$

with its slow variation of magnitude offers a contrast with the abrupt onset and end of the square pulse. This pulse has the excitation profile

$$\mathcal{S}(\Delta) = \frac{T}{\sqrt{1 + \alpha^2}} \ln \left(\frac{1 + \sqrt{1 + \alpha^2}}{\alpha} \right). \quad (27)$$

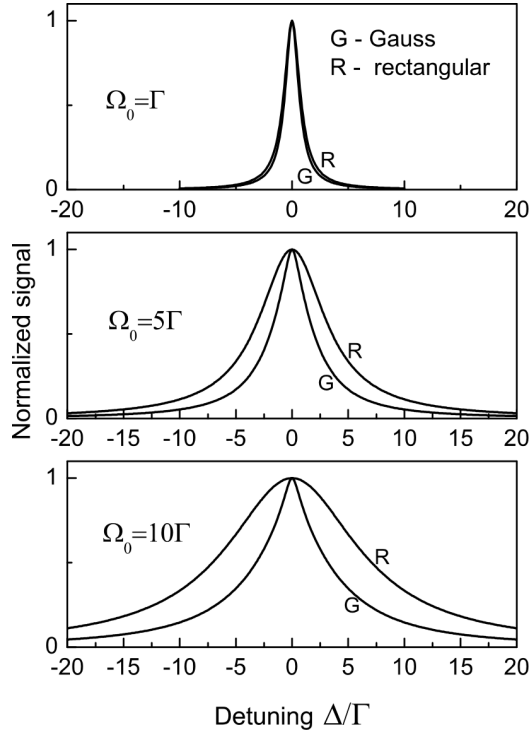


Fig. 1. Excitation profiles $S(\Delta)/S(0)$ normalized to the unit peak value vs. the detuning Δ/Γ for Gaussian pulses (G) and square pulses (R) for three values of the peak Rabi frequency, $\Omega_0 = \Gamma, 5\Gamma$ and 10Γ

The effective line width for this profile is expressible with $\alpha_0 \equiv \Gamma/\Omega_0\sqrt{2}$ as

$$\mathcal{D}(\Delta) = |\Delta| \sqrt{\frac{g(\alpha)}{g(\alpha_0)}}, \quad (28)$$

where

$$g(\alpha) \equiv \frac{\ln(1 + \sqrt{1 + \alpha^2}) - \ln(\alpha)}{\sqrt{1 + \alpha^2}}. \quad (29)$$

For small detunings, the line width is primarily determined by the natural width Γ ,

$$\mathcal{D}(\Delta) \approx \frac{\Gamma}{2} \sqrt{\ln\left(\frac{8\Omega_0^2}{\Gamma^2}\right)}, \quad (|\Delta| \ll \Gamma \ll \Omega_0). \quad (30a)$$

For intermediate detunings, the expression becomes

$$\mathcal{D}(\Delta) \approx |\Delta| \sqrt{\frac{\ln(\sqrt{2}\Omega_0/|\Delta|)}{\ln(2|\Delta|/\Gamma)}}, \quad (\Gamma \ll |\Delta| \ll \Omega_0). \quad (30b)$$

For large Δ , the width is determined by the peak Rabi frequency Ω_0 ,

$$\mathcal{D}(\Delta) \approx \frac{\Omega_0}{\sqrt{\ln(8\Omega_0^2/\Gamma^2)}}, \quad (\Gamma \ll \Omega_0 \ll |\Delta|). \quad (30c)$$

4.4. Amplitude Lorentzian pulse

Here, we consider a pulse, for which the Rabi frequency follows the time dependence

$$\Omega(t) = \frac{\Omega_0}{(t/T)^2 + 1}. \quad (31)$$

This shape provides the example of a temporal pulse with very long tails. The excitation profile

$$S(\Delta) = \frac{\pi\Gamma T\sqrt{2}}{\sqrt{\alpha(\alpha^2 + 1)(\alpha + \sqrt{\alpha^2 + 1})}}, \quad (32)$$

depends on the detuning Δ through the detuning dependence of the parameter α given by Eq. (18).

For small and intermediate detunings $\Gamma, |\Delta| \ll \Omega_0$ meaning $\alpha \ll 1$, we have

$$S(\Delta) \simeq \frac{\pi\Gamma T\sqrt{2}}{\sqrt{\alpha}}. \quad (33)$$

For this line, the effective width (12) is determined by the natural width Γ and the detuning Δ :

$$\mathcal{D}(\Delta) = \frac{\Gamma}{2} \sqrt{1 + \sqrt{1 + 4\Delta^2/\Gamma^2}}. \quad (34)$$

For a small detuning, the line width is

$$\mathcal{D}(\Delta) \approx \Gamma/2, \quad (|\Delta| \ll \Gamma \ll \Omega_0). \quad (35a)$$

For an intermediate detuning, it is

$$\mathcal{D}(\Delta) \approx \sqrt{\Gamma|\Delta|/2}, \quad (\Gamma \ll |\Delta| \ll \Omega_0). \quad (35b)$$

Using (12) and (32), it is easy to show that, for a large detuning, the width exhibits the traditional increase proportional to the square root of the peak Rabi frequency Ω_0 ,

$$\mathcal{D}(\Delta) \approx \sqrt{\Gamma\Omega_0}/2, \quad (\Gamma \ll \Omega_0 \ll |\Delta|). \quad (35c)$$

4.5. Lorentzian pulse intensity

In this subsection, we consider a pulse, whose square is a Lorentzian function, i.e. the intensity follows a Lorentzian shape

$$\Omega(t) = \frac{\Omega_0}{\sqrt{(t/T)^2 + 1}}. \quad (36)$$

It is the example of a temporal pulse with the longest tails. For this shape, the excitation profile is

$$\mathcal{S}(\Delta) = \frac{\pi\Gamma T}{2\alpha\sqrt{1 + \alpha^2}}. \quad (37)$$

For small $\alpha \ll 1$ when $\Gamma, |\Delta| \ll \Omega_0$, the excitation profile is

$$\mathcal{S}(\Delta) \simeq \frac{\pi\Gamma T}{2\alpha}. \quad (38)$$

The effective width derived from this profile is

$$\mathcal{D}(\Delta) = \frac{|\Delta|}{\sqrt{\sqrt{\left(\frac{\Delta^2}{\Gamma^2/4} + 1\right) \left(\frac{\Delta^2}{\Gamma^2/4 + \Omega_0^2/2} + 1\right)} - 1}}. \quad (39)$$

This formula has the following limits. For a small detuning, the line width is determined by the natural width Γ ,

$$\mathcal{D}(\Delta) \approx \Gamma/\sqrt{2}, \quad (|\Delta| \ll \Gamma \ll \Omega_0). \quad (40a)$$

For an intermediate detuning, the width is

$$\mathcal{D}(\Delta) \approx \sqrt{\Gamma|\Delta|/2}, \quad (\Gamma \ll |\Delta| \ll \Omega_0). \quad (40b)$$

For a large detuning, the width exhibits the traditional increase proportional to the square root of the peak Rabi frequency Ω_0 ,

$$\mathcal{D}(\Delta) \approx \sqrt{\Gamma\Omega_0/2\sqrt{2}}, \quad (\Gamma \ll \Omega_0 \ll |\Delta|). \quad (40c)$$

The hyperbolic-secant pulse and the Lorentzian pulses induce different temporal behaviors of the Bloch vector. So, it is not surprising that the resulting excitation profiles differ. Figure 2 presents a comparison of these profiles for the high peak Rabi frequencies, $\Omega_0 = 100\Gamma$, a regime where the power broadening might be expected to overwhelm the natural line width. As can be seen, even in this case, there remains a narrow central feature which, though exceeding the natural line width, is far narrower for the smooth pulses than for the square pulse.

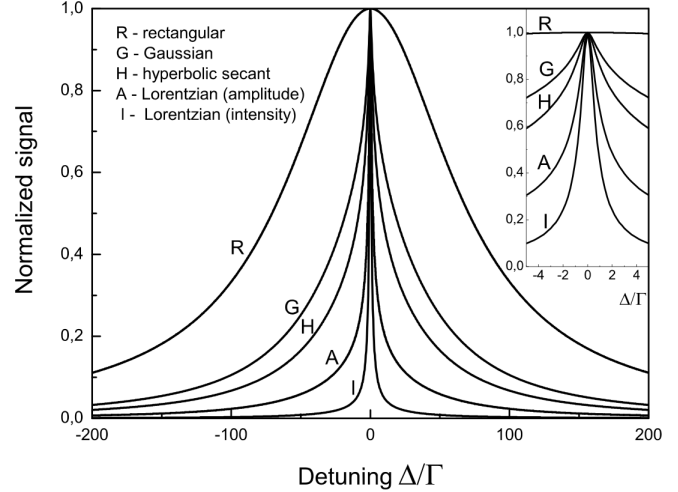


Fig. 2. Relative excitation profile $\mathcal{S}(\Delta)/\mathcal{S}(0)$ normalized to unit peak value vs. Δ/Γ for different temporal pulse shapes. The peak Rabi frequency is $\Omega_0 = 100\Gamma$

4.6. Hypergaussian

To examine the influence of the pulse shape upon the excitation profile, we have used numerical solutions of the Bloch equations for hypergaussian pulses,

$$\Omega(t) = \Omega_0 \exp(-t^n/T^n). \quad (41)$$

Figure 3 shows some examples of the excitation profile $\mathcal{S}(\Delta)$ for various temporal pulse shapes, ranging from the conventional Gaussian ($n = 2$) to the rectangular one ($n = 64$), all with the peak Rabi frequency $\Omega_0 = 100\Gamma$. We see that all of these profiles have similar wings, and the central peak becomes less pronounced as the pulse becomes more rectangular.

5. Discussion

5.1. General observations

The comparison of the line widths of pulses considered above suggests the interesting connections between the temporal pulse shape and the excitation profile. The fluorescence line of a rectangular pulse is a single Lorentzian with HWHM proportional to the peak Rabi frequency Ω_0 , Eq. (15). The fluorescence profiles of smooth pulses are more complicated [Eq. (39) for a Lorentzian pulse and Eq. (24) for a Gaussian pulse] and have different behavior near the line center and in the wings.

Near the line center, we observe a narrow feature, whose width is determined by the natural line width Γ ,

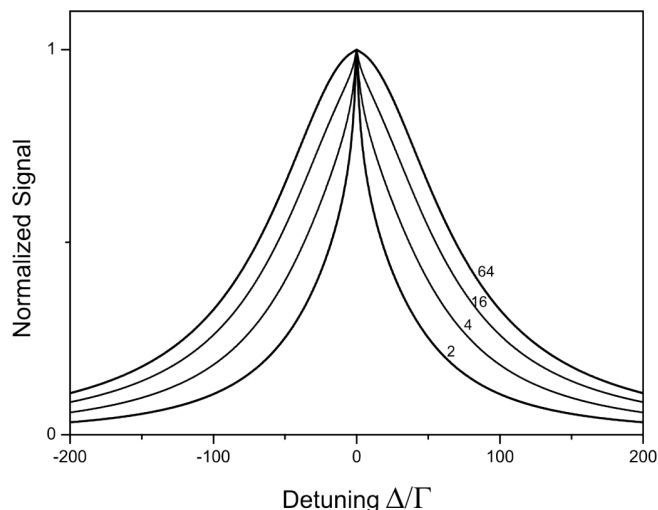


Fig. 3. Normalized excitation profile $S(\Delta)/S(0)$ vs. Δ/Γ for hypergaussian pulses $\Omega = \Omega_0 \exp(-t^{2n}/T^{2n})$ for $\Omega_0 = 100\Gamma$, for values $n = 2, 4, 16, 26$. With increasing n , the profile broadens

both for the Lorentzian pulse, Eq. (40a), and for the Gaussian pulse, Eq. (25a).

In the line wings, far from the resonance, the line width is determined primarily by the peak Rabi frequency Ω_0 . It grows in proportion to $\Omega_0^{1/2}$ for a Lorentzian pulse, whereas, for a Gaussian pulse, it grows in proportion to Ω_0

These results imply that there is a narrow feature in the fluorescence line near the line center ($\Delta = 0$). It rises from a broad “background”. The narrow feature does not exhibit the power broadening for a Lorentzian pulse and has a weak logarithmic power broadening for a Gaussian pulse. The broad background feature is power-broadened. When $\Omega_0 \gg \Gamma$, its width can exceed considerably that of the narrow central line.

The results for a rectangular pulse and smooth pulses suggest that the wide line originates from the high and nearly flat portion of the pulsed Rabi frequency $\Omega(t)$. By contrast, the narrow central feature originates from early and late times, when $\Omega(t)$ is small. Because the Lorentzian pulse has longer temporal tails, it has the more pronounced central line. The Gaussian pulse has the shorter tails, and it has the least pronounced narrow feature. The square pulse has no tails at all. Therefore, it produces no narrow line in the saturation regime ($\Omega_0 \gg \Gamma$).

It is also essential to note that, in all these examples, the excitation profiles do not depend on the pulse width T . This is in sharp contrast with the case where the excited-state population is measured *after* the excitation is completed, when the line width is determined

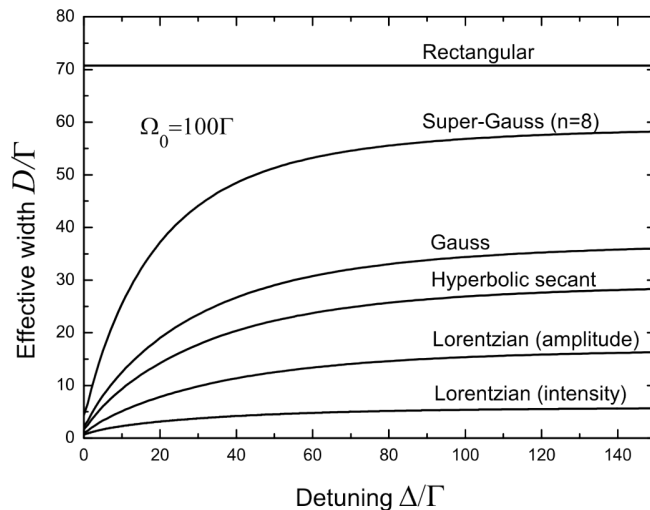


Fig. 4. Effective width $D(\Delta)/\Gamma$ vs. detuning Δ/Γ for various pulse shapes. Peak Rabi frequency is $\Omega_0 = 100\Gamma$

primarily by T , Section 2. Figures 2 and 3 illustrate this behavior.

Impressions gained from these figures are confirmed in Fig. 4. Here, we see that the effective width for a Lorentzian pulse is extremely small; it varies only slightly across the excitation profile. As pulses become more rectangular, the wings of an excitation profile broaden. But, near the line center, all these pulses have effective widths that are much smaller than the power-broadened rectangular pulse.

5.2. Influence of a deflection of atoms

The observation that the narrow feature at the line center originates from the regions of a small Rabi frequency on the tails of the pulse, along with the fact that these regions are separated in time, suggests that this narrow feature may split into components. Such a splitting can be caused by the light pressure which changes the velocity of atoms and hence induces Doppler shifts of the laser frequency in the rest frame of an atom.

The radiative force acting on an atom is

$$F(t) = \hbar k \Gamma P_2(t) = \hbar k \Gamma \frac{\Omega^2(t)/4}{\Delta^2 + (\Gamma/2)^2 + \Omega^2(t)/2}. \quad (42)$$

The change in the atom velocity v is determined by the equation

$$m \frac{dv}{dt} = F(t).$$

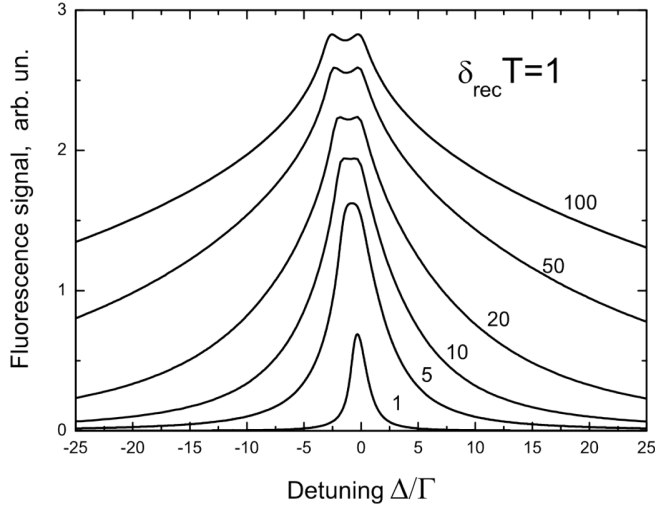


Fig. 5. Excitation profiles $S(\Delta)$ vs. the detuning Δ/Γ for various peak Rabi frequencies. $\Omega_0/\Gamma = 1, 5, 10, 20, 50, 100$. As the pulse becomes stronger, the profile becomes wider (power broadening) and a doublet structure appears at the line center

So, for the detuning $\Delta(t) = \Delta + kv(t)$, we have the differential equation

$$\frac{d\Delta(t)}{dt} = \delta\Gamma \frac{\Omega^2(t)/2}{\Delta(t)^2 + (\Gamma/2)^2 + \Omega^2(t)/2},$$

where $\delta = \hbar k^2/2m$ is the recoil frequency. For large Rabi frequencies, the magnitude of changes in the detuning is approximately $\delta\Gamma T$. Because, for a Gaussian pulse, the main contributions to the narrow fluorescence line is from early and late times, one can expect that, for a long interaction time T , this line will transform into a pair of components (a doublet) separated in frequency by about $\delta\Gamma T$. The condition for doublet observation is $\delta\Gamma T > \Gamma$ or

$$\delta T > 1.$$

Figure 5 presents excitation profiles that exhibit the appearance of a doublet as the peak Rabi frequency increases.

5.2. Conclusions

The laser-induced excitation is the strongest when the carrier frequency matches the Bohr frequency of a two-state transition, but the excitation also occurs for a near-resonant excitation. Various techniques provide possible indicators of the excitation, including signals from the photoionization and fluorescence. The range of frequencies that contribute appreciably to the excitation

signal – the width of the absorption line or the excitation profile – depends upon both the conditions of excitation and the nature of the monitoring that produces a signal. Examples presented here show that, when the excitation is pulsed, the shape of a pulse has a significant effect on the excitation profile. In particular, pulses that have long temporal tails produce a narrow feature near resonance – the center of the profile.

This work has been supported by the European Commission projects CAMEL, EMALI, and FASTQUAST, by the Bulgarian National Science Fund under grants VU-205/06 and VU-301/07 and by the National Academy of Sciences of Ukraine under grants V136, V137, and VTs139.

1. R.G. Breene, *Theories of Spectral Line Shapes* (Wiley, N.Y., 1981); I.I. Sobel'man, L.A. Vainshtein and E.A. Yukov, *Excitation of Atoms and Broadening of Spectral Lines*, (Springer, N.Y., 1995)
2. L. Allen and J.H. Eberly, *Optical Resonance and Two Level Atoms* (Dover, New York, 1975);
3. P.W. Milonni and J.H. Eberly, *Lasers* (Wiley, New York, 1988)
4. W. Demtröder, *Laser Spectroscopy: Basic Concepts and Instrumentation* (Springer, Berlin, 2003)
5. N.V. Vitanov, B.W. Shore, L. Yatsenko, K. Böhmer, T. Halfmann, T. Rickes, and K. Bergmann, *Opt. Commun.* **199**, 117 (2001).
6. T. Halfmann, T. Rickes, N. V. Vitanov, and K. Bergmann, *Opt. Commun.* **220**, 353 (2003).
7. B.W. Shore, *The Theory of Coherent Atomic Excitation* (Wiley, New York, 1990).
8. N.V. Vitanov, *J. Phys. B* **28**, L19 (1995); N.V. Vitanov and P.L. Knight., *J. Phys. B* **28**, 1905 (1995); A. Kuhn, S. Steuerwald and K. Bergmann, *Eur. Phys. J. D* **1**, 57 (1998).
9. N. Rosen and C. Zener, *Phys. Rev.* **40**, 502 (1932).
10. G.S. Vasilev and N.V. Vitanov, *Phys. Rev.* **70**, 053407 (2004).
11. B.R. Mollow, *Phys. Rev.* **188**, 1969 (1969); B.R. Mollow, *Phys. Rev. A* **2**, 76 (1970); B.R. Mollow, *Phys. Rev. A* **5**, 1522 (1972); B.R. Mollow, *Phys. Rev. A* **5**, 2217 (1972); B.R. Mollow, in *Progress in Optics XIX*, edited by E. Wolf (North-Holland, Amsterdam, 1981), pp. 1.

ФОРМА ЛІНІЙ АТОМНОГО ПОГЛИНАННЯ ЗА УМОВИ ІМПУЛЬСНОГО ЗБУДЖЕННЯ

Н.В. Вітанов, Б.У. Шоре, Л.П. Яценко

Резюме

Спектральна ширина атомних ліній поглинання, які спостерігаються за допомогою джерела неперервного когерентного світла, звичайно збільшується пропорційно квадратному кореню інтенсивності світла. Цей ефект відомий як розширення

потужністю. У даній роботі показано, що лінії, які рееструються через сигнал флуоресценції, відрізняються якісно, коли збудження є імпульсним. Розглянуто залежність сигналу флуоресценції (підсумованого за всіма частотами) від частоти випромінювання збуджуючого лазера і показано, що відповідний профіль збудження складається з двох компонент: лінії, роз-

ширеної потужністю, та вузької лінії, ширина якої залежить головним чином від натуральної ширини і тільки дуже слабо від лазерної інтенсивності. На відміну від сигналу фотоіонізації неперервним іонізуючим полем [Halfmann et al., *Opt. Commun.* 220, 353 (2003)], ширина вузької лінії не залежить від тривалості імпульсу.